

2.1.1. Singular Value decomposition (SVD)

2.1.1.1. General Singular Value decomposition (SVD)

The singular value decomposition is a widely used technique to solve ill-conditioned problems with several applications, (e.g., in image compression, watermarking, image filtering). The general SVD statement can be expressed as:

Every real matrix **A** can be decomposed into a product of three matrices of the form:

$$A = U S V^T \quad (10)$$

Where, **U** and **V** are orthogonal matrices.

On the other hand, **S** is a diagonal matrix whose elements are the singular values of the original matrix. Therefore:

$$S = \text{diag}(\sigma_1, \sigma_2, \dots, \sigma_r) \quad (11)$$

With:

$$\sigma_1 \geq \sigma_2 \geq \dots \geq \sigma_r \geq 0$$

Consequently, the inverse of **A** can be expressed as:

$$A^{-1} = V W U^T \quad (12)$$

Where **W** is also a diagonal matrix of elements $w_i = \frac{1}{s_i}$

Depending on the signal-to-noise ratio of the signal intensity function, a tolerance threshold P_{SVD} is set. The values of w_i corresponding to values where s_i is less than P_{SVD} are set to zero. Typically the threshold is given as a percentage of the greater singular value σ_1 . Generally, in MR perfusion imaging

the threshold value varies between 20 and 30% and the general principle is the higher the noise, the higher the P_{SVD} .

2.1.1.2. Singular Value decomposition adaptive threshold (aSVD)

When the SVD algorithm is used to calculate the residue function it is common to obtain a graph of the function with some non-expected oscillations. In theory, the residue function is monotone decreasing and therefore those oscillations do not have a physical sense (see **figure 02**). Liu et al. [4] showed that the P_{SVD} selection had a significant influence in the shape of the residue function and an apparently inaccuracy in the rCBF estimation. The residue function is a signal from which the blood flow is calculated and it is the one mentioned on the 4th step in section 2.1.

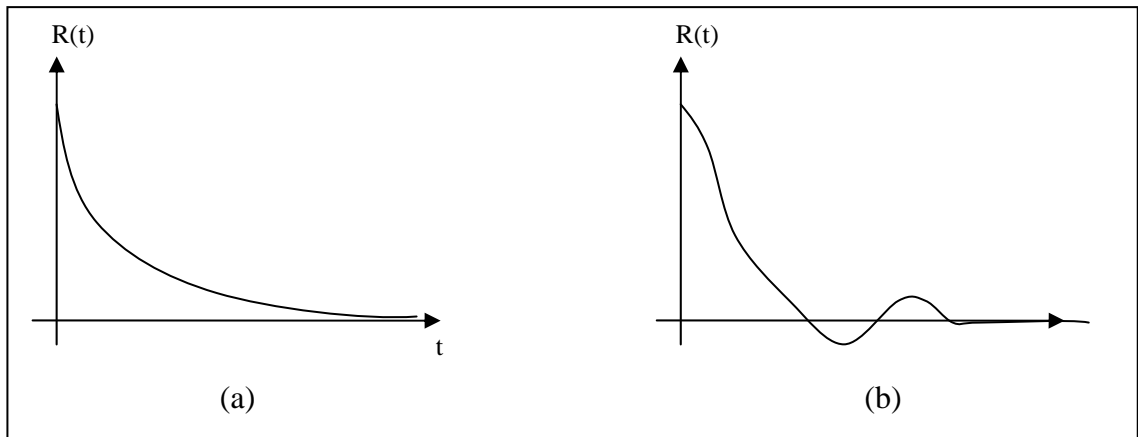


figure 02. The expected residue function (a) and the one obtained with SVD (b)

An oscillation index O , was proposed by Østergaard et al. [1] to measure the distortion in the residue function as follows:

$$O = \frac{1}{L \cdot f_{\max}} \left(\sum_{k=2}^{L-1} |f(k) - 2f(k-1) + f(k-2)| \right) \quad (13)$$

Where f is the scaled estimated residue function, f_{max} is the maximum amplitude of f , and L is the number of sample points.

This oscillation index may be viewed as the discrete form of the convolution between the residue function and the second derivative of a Gaussian distribution which is shown in **figure 03**. The use of this digital filter, which is the same as calculating the sum of the absolute value of the second derivative of $f(t)$, quantifies the change in the curvature of the function over the time.

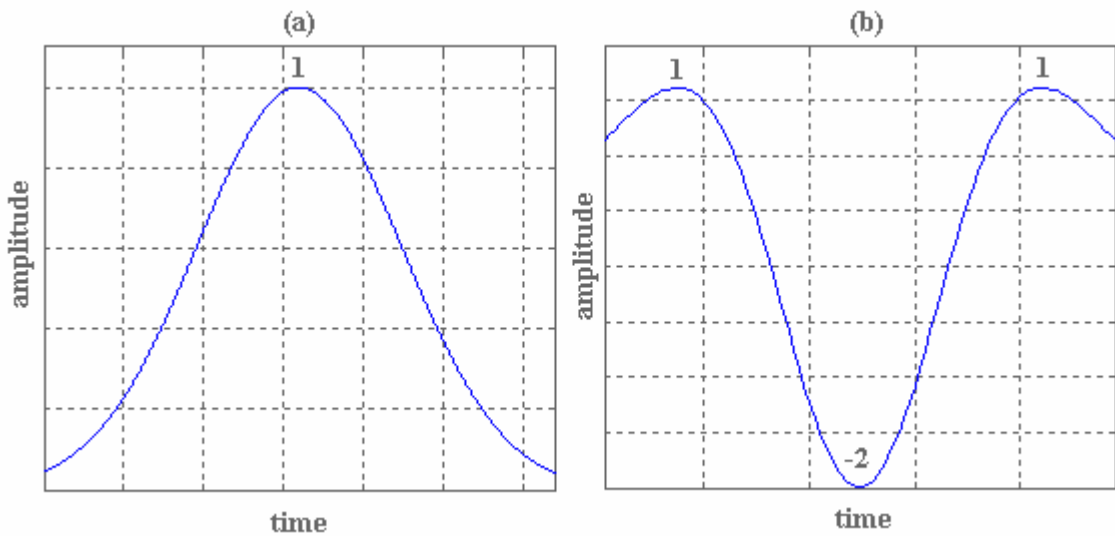


figure 03. The Gaussian distribution (a) and its second derivative (b)

As it was said before, a threshold is typically chosen between 20 and 30% in rCBF estimation, depending on the SNR of the digital image. However, it is theoretically possible to design an algorithm in which an optimum P_{SVD} is chosen automatically. The main adaptive SVD algorithm that was used in this work is shown in **figure 04**. Again, it can be summarized in a step-by-step procedure as follows:

- I. The lower value of the P_{SVD} threshold is initialized.

- II. The residue function is calculated using the SVD deconvolution method.
- III. The oscillation index O of the correspondent residue function is calculated.
- IV. The P_{SVD} threshold value is incremented.
- V. The process is repeated from step II until the upper value of the P_{SVD} threshold is reached.
- VI. The residue function which has the minimum oscillation index O is selected and the rCBF is calculated using O_{min} .

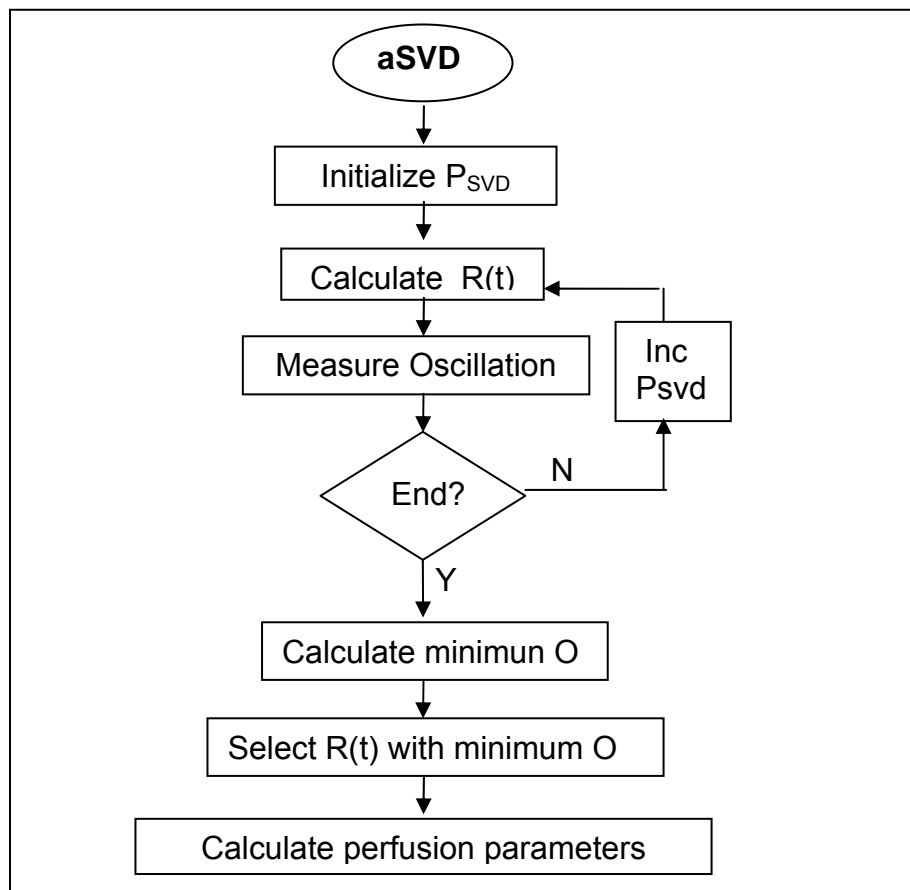


figure 04. Adaptive SVD algorithm

2.1.2. Auto Regressive Moving Average (ARMA)

ARMA is the second method of deconvolution used in this work to estimate the rCBF. As is was noted earlier, to calculate the blood flow it is necessary to calculate a specific function denoted $r(t)$ -more specifically the discrete form $r(n)$ because the sequence of images is discrete-. The estimation of this residue function $r(n)$ can be treated as a spectral parametric analysis problem. One way of solving this kind of problems is presented here from the system theory point of view and showing its basic mathematical statements.

It is known that when a linear time-invariant (LTI) system is excited by the Dirac's delta function, the output is the transfer function of the system.

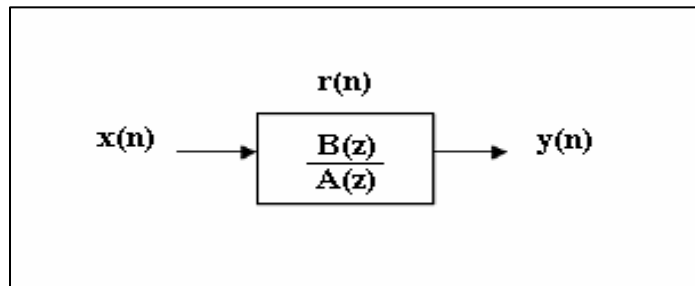


figure 05. Discrete time ARMA model representation

The discrete time filtering theory states that the impulse response of a linear system $h(n)$ can be modeled using one of the following frequency responses:

- I. The “zeros model” or moving average (MA):

$$H(z) = B(z) \quad (14)$$

II. The “poles model” or autoregressive (AR):

$$H(z) = \frac{1}{A(z)} \quad (15)$$

III. And the “zeros and poles” model (ARMA):

$$H(z) = \frac{B(z)}{A(z)} \quad (16)$$

This last model (III) is the one used and as its name suggest, it is presented as the ratio of poles and zeros in the Z-transform. Therefore equation (16) becomes:

$$H(z) = \frac{\sum_{k=0}^M b_k \cdot z^{-k}}{1 - \sum_{l=1}^N a_l \cdot z^{-l}} \quad (17)$$

The aim of the ARMA technique modeling is to find the transfer function $H(z)$, whose impulse response $h(n)$ approximates the scaled tissue response $r(n)$, such that the sum of the squared error, denoted e , is minimum:

$$e = \sum [h(n) - r(n)]^2 \quad (18)$$

Considering the system illustrated in **figure 05**, and using the ARMA model, the output $y(n)$ is computed as:

$$y[n] = \sum_{l=1}^N -a_l \cdot y[n-l] + \sum_{k=0}^M b_k \cdot x[n-k] \quad (19)$$

This mathematical statement generates a set of simultaneous equations:

$$\left\{ \begin{array}{l} y(0) = -a_1 y(-1) - a_2 y(-2) - \dots - a_n y(-n) + b_0 x(0) + b_1 x(-1) + \dots + b_m x(-m) \\ y(1) = -a_1 y(0) - a_2 y(-1) - \dots - a_n y(1-n) + b_0 x(1) + b_1 x(0) + \dots + b_m x(1-m) \\ \vdots \\ y(N-1) = -a_1 y(N-2) - a_2 y(N-3) - \dots - a_n y(N-1-n) + b_0 x(N-1) \\ \quad + b_1 x(N-2) + \dots + b_m x(N-1-m) \end{array} \right. \quad (20)$$

This can be compactly expressed, in matrix notation as

$$Y = A\Theta \quad (21)$$

where \mathbf{Y} represents the output matrix, \mathbf{A} is the input-output matrix and Θ is the ARMA parameter matrix (coefficients a_k and b_k).

Therefore, this general ARMA-model matricial representation is written as

$$\begin{pmatrix} y(0) \\ y(1) \\ \vdots \\ y(N-2) \\ y(N-1) \end{pmatrix} = \begin{pmatrix} x(0) & x(-1) & \dots & x(-m) & y(-1) & y(-2) \dots & y(-n) \\ x(1) & x(0) & \dots & x(1-m) & y(0) & y(-1) \dots & y(1-n) \\ x(2) & x(1) & \dots & x(2-m) & y(1) & y(0) \dots & y(2-n) \\ \vdots & \dots & \dots & \dots & \dots & \dots & \vdots \\ x(N-2) & x(N-3) & \dots & x(N-2-m) & y(N-3) & y(N-4) \dots & y(N-2-n) \\ x(N-1) & x(N-2) & \dots & x(N-1-m) & y(N-2) & y(N-3) \dots & y(N-1-n) \end{pmatrix} \begin{pmatrix} b_0 \\ \vdots \\ b_m \\ -a_1 \\ \vdots \\ -a_n \end{pmatrix}$$

To solve the linear equations system $Y = A\Theta$, an estimation square error is defined as

$$SE = e e^T$$

where $e = Y - A\Theta$

The minimization of the error by the least mean square process gives the coefficients a_i and b_i , and consequently the searched solution.

$$\hat{\Theta} = \arg[\min(Q_{LMS}(\Theta))] \quad (22)$$

Where $Q_{LMS}(\Theta) = \|Y - A\Theta\|^2$

To minimize this equation the SE must be differentiated with respect to Θ and equated to zero.

$$\frac{\partial SE}{\partial \Theta} = 0 \quad (23)$$

Solving equation (23) :

$$\hat{\Theta} = (A^T A)^{-1} A^T Y \quad (24)$$

Where Θ represents the unknown ARMA parameters and the solution of the deconvolution problem needed to estimate the rCBF.

2.2. Biological system modeling

2.2.1. The human body model as a dynamic system

The physiological behavior of some organs can be modeled using the dynamic systems theory. The heart, veins, arteries and capillaries may be treated as a biological system which can be mathematically represented, where variables and parameters interact regularly. This representation provides a powerful tool to estimate variables when some parameters are unknown.

Another advantage of the dynamic systems theory is that various -apparently different- physical parameters (e.g., temperature, flow, concentration and voltage) can be handled without modifying the equation's essence. In recent

years, the study field for new concepts such as the biochemical circuit theory analysis is today a fundamental field of interest for many laboratories.

The physical elements treated in this medical context, are the perfusion parameters, i.e., regional cerebral blood flow rCBF, regional cerebral blood volume rCBV, mean transit time MTT. However, the same parameters and relationships can be deduced and applied in a different area such as the myocardial circulatory system. In the published literature, the notation is quite similar except for that the letter M (myocardial) replaces the letter C (cerebral), in the perfusion parameter abbreviations.

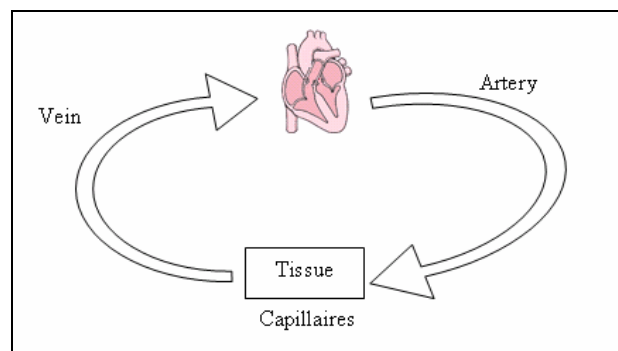


figure 06. Simplified blood circulation scheme

The human circulatory system is divided into two main parts with the heart acting as a double pump. This organ pumps a special kind of fluid, which is the blood. The across variable in this case, the blood flow, leaves the left side of the pump (heart) and travels through arteries which gradually divide into capillaries. In the capillaries, the nutrients are released to the body cells. The blood then travels in veins back to the right side of the pump, and the whole process begins again. The human simplified blood circulation process is shown in **figure 06.**

To determine if a specific human tissue is correctly irrigated, the artery tissue exchange process must be analyzed. To this aim, several approaches have

been developed. One of the most common ways in which this kind of process is analytically described is the black-box model which is shown in **figure 07**. This model is not only used to describe electrical circuits, communication systems but it is also seen as suitable mathematical approach to physiological processes such as the circulatory system. Usually, the black-model description is used to predict the output of a system for a particular input when the transfer function is known.

Supposing that the input of a certain system **H** is **X**, the output **Y** can be calculated as:

$$Y = X \otimes H \quad (25)$$

Where \otimes denotes the convolution operator.

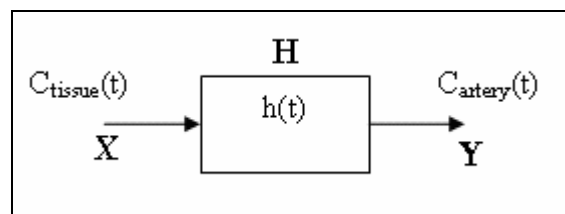


figure 07. Perfusion black-model approach.

If **X** and **Y** represent respectively the arterial and tissular concentration of the system with transfer function **H**, the equation (25) may be rewritten as:

$$C_{tissue}(t) = C_{artery}(t) \otimes h(t) \quad (26)$$

However, in MR perfusion imaging the transfer function of human organs is rarely known, therefore the convolution approach is not directly used. However, using the MR images it is possible to indirectly measure the arterial and tissular concentrations. Therefore, knowing $C_{tissue}(t)$ and $C_{artery}(t)$ it is possible to

calculate an approximation of the transfer function $h(t)$ using one of the deconvolution methods explained in the previous section. The estimation of $h(t)$ as it will be explained later, will lead to the estimation of the residue function and consequently to the rCBF measure.

The biodynamic system has the following components:

- Parameters: the rCBF and rCBV.
- Dependent variables: the arterial, tissular and venous concentration, denoted C_a , C_t and C_v respectively.
- Independent variable: the time.

2.2.2. The Stewart-Hamilton model

The Stewart-Hamilton model applied to MRI acquisition techniques can help estimate perfusion parameters such as the regional cerebral blood flow rCBF, mean transit time MTT or regional cerebral blood volume rCBV, describing the tissue condition.

The concentration of tracer within a tissular volume, at a given time t , during the passage of a bolus injection of a contrast agent, is given by:

$$C_{tissue}(t) = \rho \cdot rCBF \cdot R(t) \otimes C_{artery}(t) \quad (27)$$

Where ρ denotes the tissue density (i.e., the tissue mass per unit volume), C_{artery} is the arterial concentration and $R(t)$ is the residue function and represents the tissular retention of the contrast agent.

If this biodynamic system has a single fluid storage element hence, the residue function can be treated as the response of a first-order circuit. The general solution for this differential equation is of the form:

$$R(t) = K \cdot e^{-\frac{t}{\tau}} \quad (28)$$

In MR perfusion imaging, K is equal to one and τ is usually replaced by the mean transit time constant, denoted MTT . This value is considered as the mean time taken by the blood to pass through the system, from the arterial entrance to the vascular exit.

Let

$$r(t) = rCBF \cdot R(t) \quad (29)$$

Where $r(t)$ is a scaled residue function.

Therefore, one way to know the rCBF is evaluating the scaled residue in zero:

$$rCBF = r(0) \quad (30)$$

Assuming the tissular density being close to the water density, i.e.,

$$\rho \approx \rho_0 = 1 \frac{g}{ml},$$

Then the equation (27) becomes:

$$C_{tissue}(t) = r(t) \otimes C_{artery}(t) \quad (31)$$

Once the regional blood flow is estimated, the unknown perfusion parameters, can be computed from the central volume theorem (Stewart, 1984; Meier and Zierler, 1954):

$$rCBF = \frac{rCBV}{MTT} \quad (32)$$

where rCBV and MTT are the regional cerebral blood and mean transit time, respectively and

$$MTT = \int_0^{\infty} R(t) dt \quad (33)$$

However, the concentration is measured from the MR digital images, therefore, the continuous time form of the previous equations is not considered. In consequence, the Stewart-Hamilton model becomes a discrete convolution:

$$C_{tissue}(k) = \sum_{i=0}^k C_{artery}(i) \cdot r(k-i) \quad (34)$$

Moreover, the discrete convolution can be viewed as a matricial product:

$$\begin{pmatrix} C_{tissue}(0) \\ C_{tissue}(1) \\ \dots \\ C_{tissue}(N) \end{pmatrix} = \begin{pmatrix} C_{artery}(0) & 0 & \dots & \dots & 0 \\ C_{artery}(1) & C_{artery}(0) & 0 & \dots & \vdots \\ \dots & \dots & \dots & \dots & \dots \\ C_{artery}(N) & C_{artery}(N-1) & \dots & \dots & C_{artery}(0) \end{pmatrix} \begin{pmatrix} r(0) \\ r(1) \\ \cdot \\ \dots \\ r(N) \end{pmatrix}$$

Where N is the number of samples taken in the RM sequence.

This product can be compactly denoted as:

$$T = A \Gamma \quad (35)$$

Where Γ is unknown.

Hence, the deconvolution process becomes a linear algebra problem, specifically, a matrix inversion problem:

$$\Gamma = A^{-1} T \quad (36)$$

However, this process, when working with noisy signals, could sometimes lead to determinants close to zero, the matrix A is said to be “ill-conditioned”, and consequently, unexpected results may be obtained. For this reason, a robust deconvolution method such like the ones exposed in section 2.1 must be used.

Moreover, the concentration of the contrast agent is not directly measured in clinical practice; instead, MR images are used to determine signal intensity (SI) variations over time, which are related with the change in the spin-spin relaxation -also known as the transverse relaxation (ΔR_2^*)-. The SI functions are obtained by selecting a pixel or a region of interest (ROI) in the MR gray-scale digital images.

Previous studies have shown the existence of a linear relation between the measured concentration C(t) and ΔR_2^* .

$$C(t) \propto \Delta R_2^* \quad (37)$$

On the other hand, the transverse relaxation and the signal intensity have an exponential dependence. The main relation can be written as follows:

$$C(t) = -K \cdot \frac{1}{TE} \ln \frac{SI(t)}{S_0} \quad (38)$$

Where TE is the sequence echo time, SI(t) is the signal intensity over time and S_0 is the baseline MR intensity. Consequently, by measuring SI_{tissue} and SI_{aif} the regional blood flow can be estimated using a deconvolution technique and evaluating the expression r(t) at zero. The main process is summarized in **figure 08**.

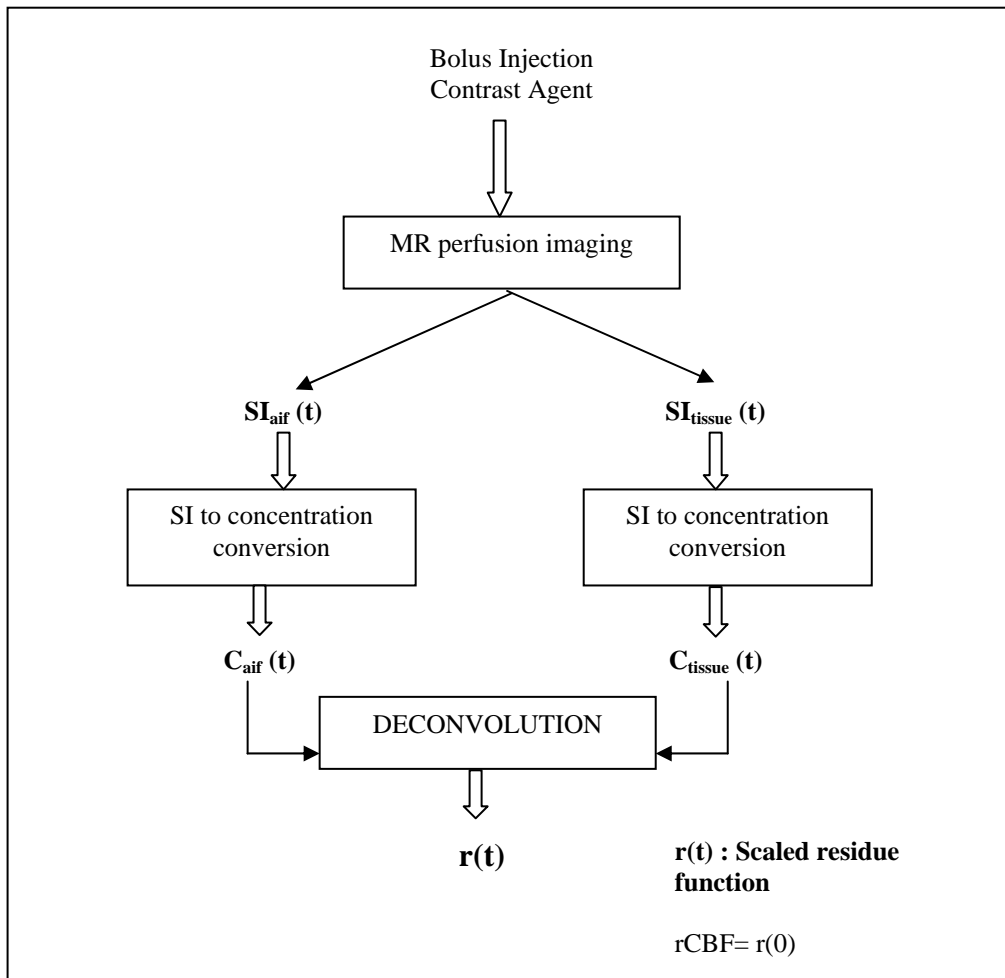


figure 08. Parameter estimation procedure using MR perfusion imaging

2.3. Sample size selection in statistical experiments

In the present work, it is desired to know which of the two deconvolution methods is more appropriate to cerebral blood flow estimation. The first part of the experiment consisted in simulating the MR signals using the MATLAB software. However, the first problem appeared when it was necessary to choose the number of samples in order to obtain statistical data. The statistical data was needed to make the mathematical comparison of the ARMA, SVD and aSVD deconvolution methods.

Nevertheless, the sample size selection is not an arbitrary decision; it is necessary to know the maximum error allowed in the clinical context and to have a general idea of estimation theory to determine it. Demonstrations and more detailed information on the principles in population size selection can be found in the probability and statistics literature [10]. A basic review on the theory is presented here to help to non-familiarized readers, since its misunderstanding is usually a source of inaccuracies in system-modeling simulations.

The present experiment is very similar to the situation of political polls, designed for example, to determine who is the most likely to be president between two candidates. As it is known, polls are not error free and most of the time, the number of votes counted after the elections, is not exactly the same as the predicted by the official survey. However polls are used world wide since they are useful not only in politics but in economy, sociology and many other fields. A mayor issue in a survey is the selection of the population size, in order to obtain a specific error that can be measured. In other words, it is wanted to know how confident the poll is.

Of course, different fields require different precision, so the first thing that should be known is the minimum number that is significant for a specific

context. In the politician election example, suppose that we a sample size of 100 000 random citizens is selected in the poll. Results show candidate **A** with 30% of the votes and candidate **B** with 40%, now suppose that more precision is wanted, so the sample size is doubled. The second poll now shows candidate **A** with 29% and candidate **B** with 43% of the votes. It is clear that it was not worth to double the sample size since both polls are giving almost the same information, i.e., candidate **B** is more likely to win the elections. However, time and money spent on the second poll was almost certainly greater than the one on the first poll. Therefore, a difference of ± 1 vote is not crucial, except on the special case where candidates tie. However in the medical context, a difference of ± 1 ml/s in cerebral blood flow assessment can be crucial, especially if the life of the patient depends on the correct estimation of this perfusion parameter.

Consequently, mathematicians have developed techniques to calculate the sample size of an experiment to obtain a certain degree of precision, in other words, a confidence interval. However, the population size selection is dependent of the standard deviation and most of the time, this parameter is unknown. Therefore, it is necessary to select an arbitrary sample size (N) in the beginning (habitually $N > 30$) and then calculate the sample standard deviation (SSD). However for simplicity, the SSD will be just denoted from now on, as the standard deviation (SD). Assuming a normal distribution:

$$SD \cong SSD = \sqrt{\frac{\sum_{i=1}^N (x_i - \bar{x})^2}{N}} \quad (39)$$

Where \bar{x} is the arithmetic mean of the set of samples.

Once, the SD of the population sample is calculated, N can be determined with the following theorem:

“We can be $(1 - \alpha) \cdot 100\%$ confident that the error will be less than a specified amount e when the sample size is:

$$N = \left(\frac{Z_{\alpha/2} \cdot SD}{e} \right)^2 \quad (40)$$

Where $Z_{\alpha/2}$ is the value of the standard normal distribution leaving an area of $\alpha/2$ to the right. ”

3. METHODS

With the increasing software and hardware advances, computer simulation is today seen as an extremely powerful and useful tool in modern science research. Uncountable experiments are performed using random computer simulations in many different fields such as economy, acoustics, weather forecasting, sociology, medicine, engineering, etc.

The main purpose of these simulations is to recreate a virtual environment in which an experiment is done. The same action in the same experiment conditions is often repeated an elevated number of times in order to analyze its statistical properties. This kind of statistical sampling techniques using computers simulations is frequently known in the scientific literature, as the Monte-Carlo methods. There are several historical explanations of the use of this expression. In general, it is believed this term was first used by the Polish-American mathematician, Stanisław Marcin Ulam. The Monte-Carlo area (Principality of Monaco) is well known for its gambling and casinos and apparently, the phrase was given in honor of Ulam's uncle who was a gambler. In the present work, the name of Monte-Carlo simulations was used to describe the first part of the deconvolution experiment in which computer tools were applied. A basic description of the Monte-Carlo methods used in this text is presented in this section.

3.1. Monte–Carlo simulations

In order to assess the performance of the different deconvolution techniques, realistic MR signals were generated. The statistical data sample of the Monte Carlo simulation was the estimated regional blood flow, which was calculated from noisy concentration functions. These simulated signals were considered as a suitable approximation of what is typically measured in patients.

3.1.1. Range of simulated perfusion parameters

Representative rCBF values were selected from the scientific literature [1]. The rCBF range varying from 5 to 35 ml/100g/min in 5 ml/100g/min increments was chosen for a volume rCBV = 2%, corresponding to healthy white matter. Afterwards, the rCBF was used to calculate the MTT characteristic values, applying the central volume theorem (32).

The same process was used for rCBV=4%, corresponding to healthy gray matter, except for that the range varied from 10 to 70 ml/100g/min, in 10 ml/100g/min increments. These values are summarized in the following table.

MTT (s)	24	12	8	6	4,8	4	3,43
rCBF(ml/100g/min) RBV=2%	5	10	15	20	25	30	35
rCBF(ml/100g/min) RBV=4%	10	20	30	40	50	60	70

table 1. Simulated perfusion parameters. Mean transit time, regional blood flow and regional blood volume.

3.1.2. Noisy MR signals simulation procedure

In order to simulate each of the rCBF in both blood volumes values (i.e., rCBV= 2% and rCBV= 4%), the following procedure was applied:

First, the simulated residue functions were generated as:

$$R_{sim}(t) = e^{\frac{-t}{MTT_{sim}}} \quad (41)$$

for each of the 14 different rCBF values.

The arterial input function (AIF) was simulated as a gamma-variate function

$$AIF = C_{aif}(t) = C_{peak} \cdot \left(\frac{t}{\tau}\right)^{\alpha} \cdot e^{\frac{-\alpha t}{\tau} + \alpha} \cdot u(t) \quad (42)$$

where $u(t)$ is the step function (due to causality in the modeled system).

The concentration tissue response $C(t)$ was then obtained by convolving the AIF with each residue function -equation (31)-. The signal intensity functions (SI) were calculated assuming an exponential relationship between $C(t)$ and the pixel gray-level, as it was exposed in equation (38). Solving this equation, for $SI(t)$:

$$SI(t) = S_0 e^{-k C(t)TE} \quad (43) \quad (43) \quad 50A8>0>Tj12.00439 n$$

to a typical region of interest (ROI). It is very important to notice, that the noise can not be directly added to the concentration functions since the existence of a non linear relationship between $C(t)$ and the simulated signal intensities.

To simplify the notation, let the function Ψ' be the noisy version of Ψ :

$$\Psi'(t) = \Psi_{noisy}(t)$$

Once the noisy SI functions were generated, arterial and tissue concentrations were calculated using equation (38), which is the inverse of equation (43).

Therefore, the arterial conc

Every deconvolution method was tested in the 7 different blood flows values and the number of replicates for each one, denoted N, was of 150.

3.1.4. Deconvolution performance criteria

The mean of the simulated samples, for each of the estimated rCBF, was calculated and subsequently compared with the true values (see **table 1**).

To evaluate the performance of the deconvolution techniques, the percentage error (PE) and the standard deviation was calculated for different rCBF and blood volumes. The standard deviation for a discrete variable made up of N observations is the positive square root of the variance and is defined as:

$$SD = \sqrt{\frac{\sum_{i=1}^N (x_i - \bar{x})^2}{N}}$$

where \bar{x} is the arithmetic mean of the set of samples and N=150.

The mean percentage error, denoted MPE, was defined as follows:

$$MPE = \frac{1}{N} \sum_{i=1}^N PE_i$$

where N is the number of simulated flows and,

$$PE = 100 \cdot \frac{rCBF_{identified} - rCBF_{true}}{rCBF_{true}} \quad (48)$$

However, the deconvolution performance was not only assessed in terms of its error and standard deviation. Sensibility to SNR shifts or to sample rate was also considered in the analysis.

3.1.5. ARMA vs. SVD

The first part of the simulation was the comparison of the ARMA and the SVD deconvolution in the cerebral perfusion context. Similar studies have been done in the myocardial environment [2], so different blood flow ranges are found in this project. Moreover, the sample rate was included as an additional issue in the analysis and it was tested in different noisy environments. The different simulation environments are summarized in **figure 10**. For the ARMA deconvolution algorithm, a first poles-model order and a second order for the zeros-model was used. On the other hand, a fixed 30% threshold was first chosen for the SVD method.

Two distinct tissular signal-to-noise ratios were used, in order to simulate an approximated realistic random noise when using single pixel or ROI selection. The pixel and ROI SNR are two simulated levels of noise and they recreate an approximation of the different real noise environments depending on whether the user selects a single pixel or a group of pixels. An example of ROI or pixel selection in perfusion MR imaging is illustrated in **figure 09**. To calculate the rCBF, the user must first select an option, denoted **Op**, from two possibilities: ROI or P. Depending on the selected **Op**, the area of interest **A_{Selected}** in the MR image, will be a set of pixels **S** or a single pixel **P**:

$$A_{Selected} = \begin{cases} S = \left\{ \bigcup_{j=1}^N Pixel_j \right\} & \text{if } Op = ROI \\ P = Pixel_x & \text{if } Op = P \end{cases}$$

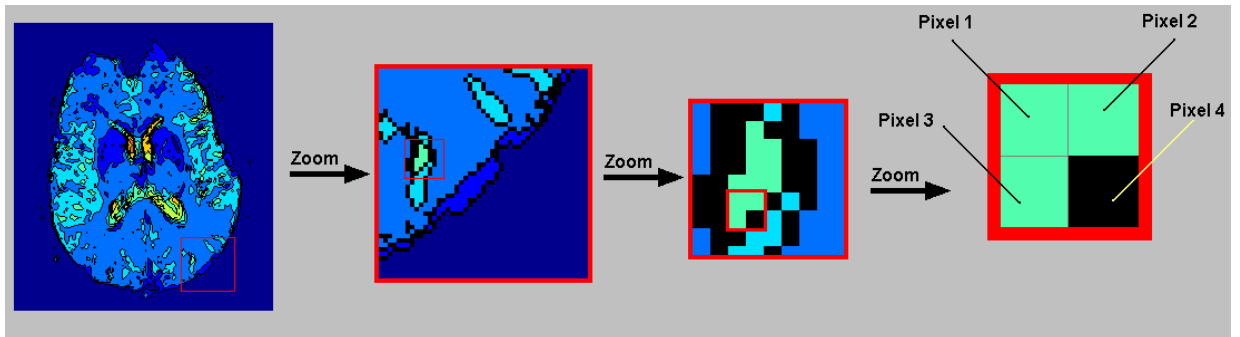


figure 09. Example of pixel or ROI selection in MR images. The user can select a set of pixels (ROI) or a single pixel (P) in rCBF estimation (e.g., ROI= Pixel 1+Pixel 2+ Pixel3 or P=Pixel 4)

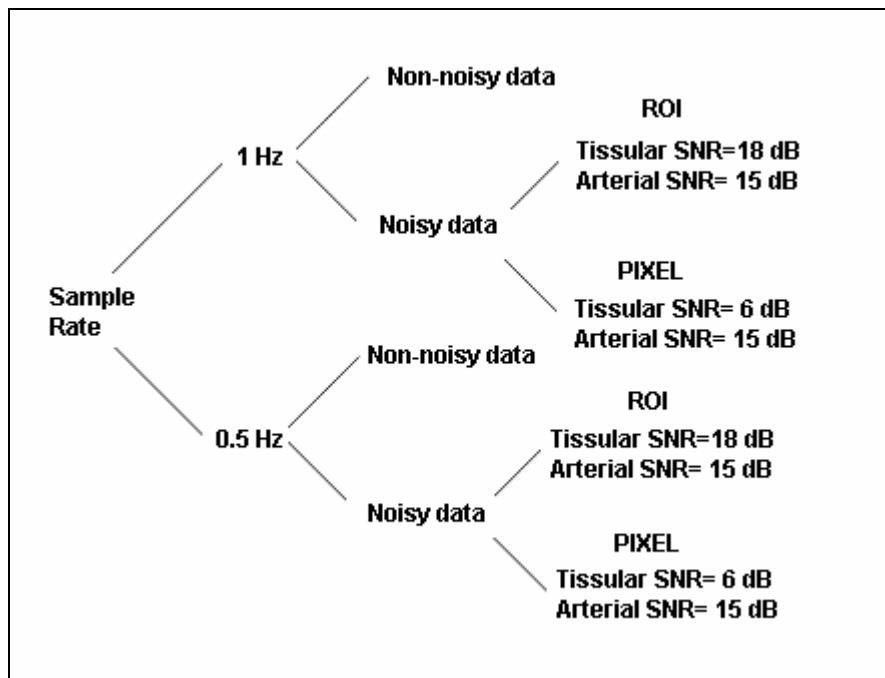


figure 10. ARMA vs. SVD perfusion simulation strategy.

3.1.6. SVD vs. adaptive threshold SVD

The adaptive threshold SVD deconvolution (aSVD) performance was tested and compared with the non-adaptive method for a sampling rate of 1 Hz in two different noisy environments, as shown in the following scheme:

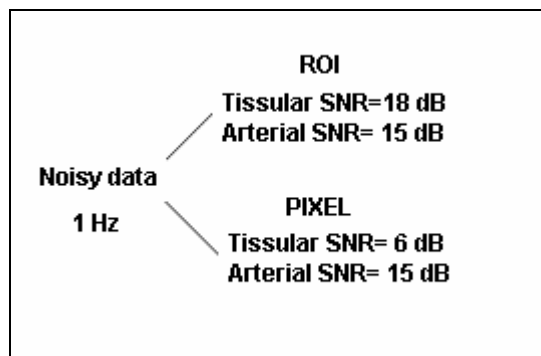


figure 11. SVD vs. aSVD perfusion simulation strategy.

The percentage threshold was first set at 30 % and then the oscillation index was calculated. The aSVD algorithm consisted in systematically changing the P_{SVD} in the range [20% , 40%] in 4 % increments in order to recalculate the respectively oscillation index of the residue functions. Afterwards, all the oscillation indexes were compared and the minimum was selected. The residue function having this minimum oscillation index is then used to calculate the desired perfusion parameters. The reader can refer to section 2.1.1.2. to obtain the detailed description of the adaptive SVD algorithm.

3.2. Perfusion MRI in stroke patients

Patients and image acquisition

Nineteen patients (age range, 32-94) with symptoms of acute hemispheric stroke were retrospectively included in the present study, observing all respective medical and ethical regulations.

MRI studies were obtained within 6 hours from symptom onset using a 1.5-T Magnetom Vision whole body MR imager (Siemens, Erlangen, Germany). Perfusion-weighted MRI was performed with a T2*-weighted gradient-echo echo-planar imaging sequence, using the bolus passage of contrast agent (repetition time: 2000 ms; echo time: 60ms; 7 slices; slice thickness: 5 mm; interslice gap: 0.5 mm; field of view: 240 mm; matrix 128 x 128 voxels; 30 measurements obtained at intervals of 2s).

The contrast injection (15 ml of Gd-DTPA) was performed after the third scan, using a power injector at a rate of 5 ml/s via access through an antecubital vein; the bolus of contrast medium was followed by a 15-ml bolus of saline solution at the same injection rate.

Data post-processing

Perfusion data were transferred onto an independent work-station and analyzed using homemade programs written in Matlab language (Math Works, Natick, MA). To obtain the SI functions, tissular and arterial ROIs were manually selected and converted to concentration signals applying the logarithmic relationship (43). The cerebral blood flow estimation was then calculated using the ARMA and SVD deconvolution techniques (46).

4. RESULTS AND DISCUSSION

4.1. Monte-Carlo simulations

4.1.1. ARMA vs. SVD

Sampling Rate: 1 Hz (1 sample per second)

Non-noisy data

In the case of non-noisy data for a PSVD threshold of 30%, the SVD estimated flow was underestimated. The mean percentage error was -34% . In contrast, using the ARMA deconvolution, the true and identified cerebral blood flows were identical for both blood volume values hence the percentage error was 0%. The rCBF estimation results are shown in the following figure:

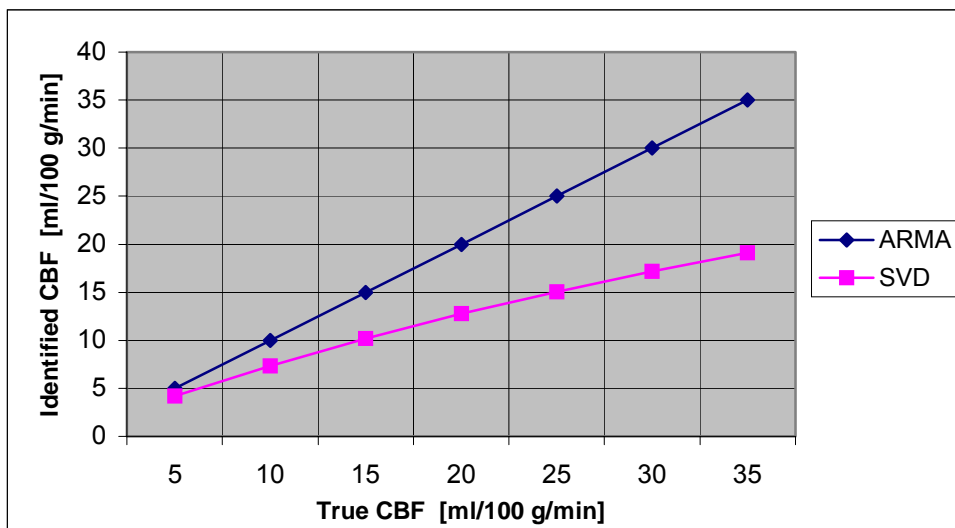


figure 12. rCBF estimation without random noise using ARMA and the SVD deconvolution ($P_{\text{SVD}} = 30\%$).

The estimation in a non-noisy environment was used to show the influence of the Psvd percentage threshold selection in blood flow estimation. The underestimation in the SVD method was due to the elimination of the lower singular values that contain non-noisy information in the matrix. Those elements are not supposed to be removed without the presence of random noise. Obviously, if a small (close to zero) Psvd percentage threshold had been chosen, both results would have been the same. The variation effect of this parameter is shown in **figure 13**. Note that the appropriate Psvd for a high SNR tends to zero.

Noisy data in ROI simulation

For $\text{SNR}_{\text{tis}} = 18$ dB and $\text{SNR}_{\text{aif}} = 15$ dB the identified rCBF was underestimated in the ARMA simulation, with a mean percentage error of -6.9% and a mean standard deviation of 5.8. In SVD, there was also an underestimation; however, the absolute value of the mean percentage error was greater than the ARMA one. On the other hand, the standard deviation of the SVD was less than the ARMA one. This phenomenon was valid for both blood volumes as illustrated in **figure 14**.

Noisy data in pixel simulation

When the tissular SNR was decreased to 6 dB without changing the arterial signal-to-noise ratio ($\text{SNR}_{\text{aif}} = 15$ dB) the calculated data was, in this case, overestimated using the ARMA model with a mean percentage error of $+86\%$.

On the contrary, the identified CBF with the SVD deconvolution technique remained underestimated with a mean percentage error of -34.5% .

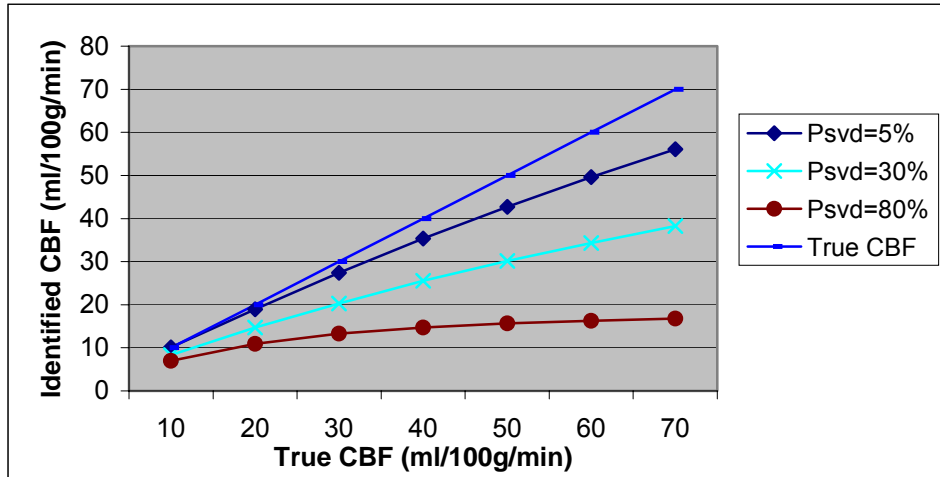


figure 13. Influence of Psvd threshold selection in flow estimation without random noise in SVD deconvolution method.

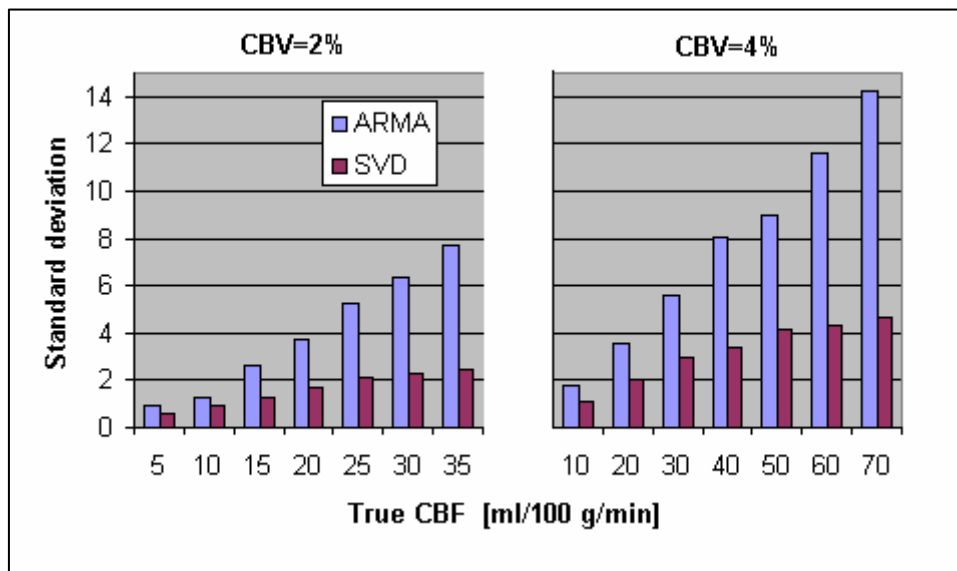


figure 14. Standard deviation comparison for ARMA and SVD. (R=1Hz, SNRtis= 18 dB and SNRaif = 15 dB).

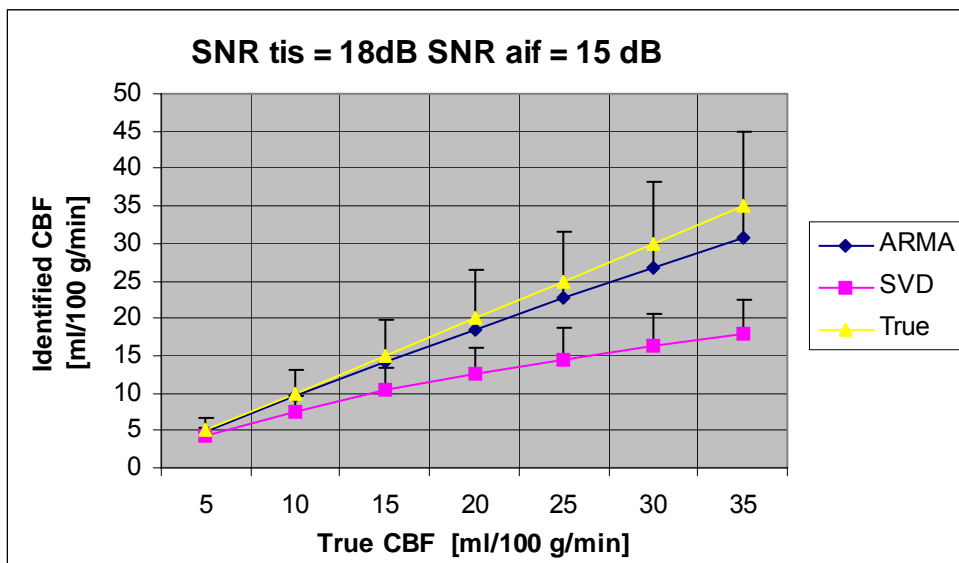
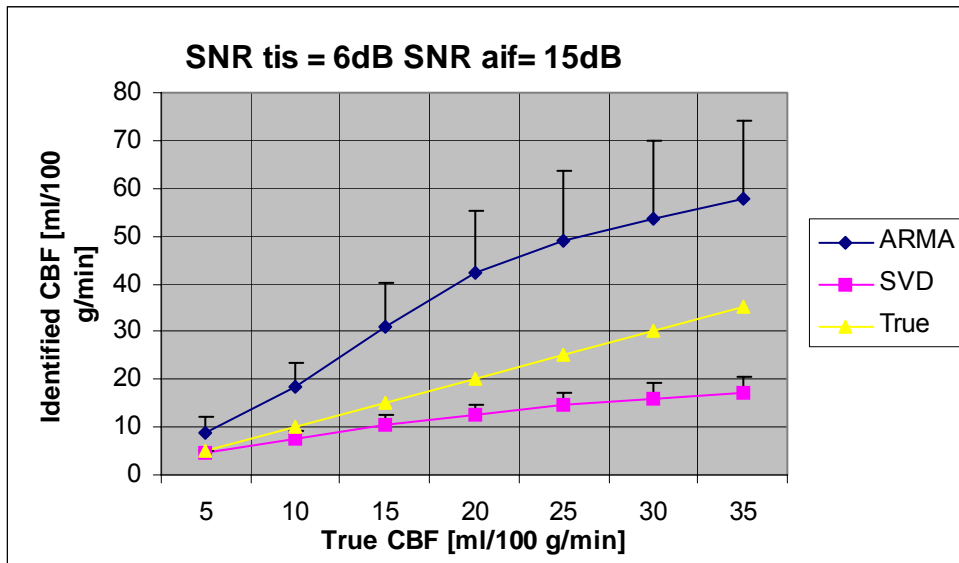


figure 15. This figure illustrates the SNR shift sensitivity in flow estimation using both deconvolution methods (rCBV=2% and sampling rate of 1Hz.)

Sampling Rate: $R_s = 0.5$ Hz (1 sample every 2 seconds)

Non-noisy data

When the sample rate was halved, there was no significant change in the rCBF estimation. The performance without the presence of random noise for $R_s = 0.5$ Hz, was similar for both techniques. That means a zero mean percentage error (MPE) using ARMA and a variable MPE in the SVD deconvolution, depending on the selected threshold:

$$MPE_{SVD} \approx 0 \text{ if } P_{SVD} \rightarrow 0\%$$

Noisy data in ROI simulation

Sensitivity to sample rate shift:

The estimated blood values that were first underestimated in the ROI SNR, for $R_s = 1$ Hz in both deconvolution methods changed to overestimation, when the sample rate was halved to $R_s = 0.5$ Hz.

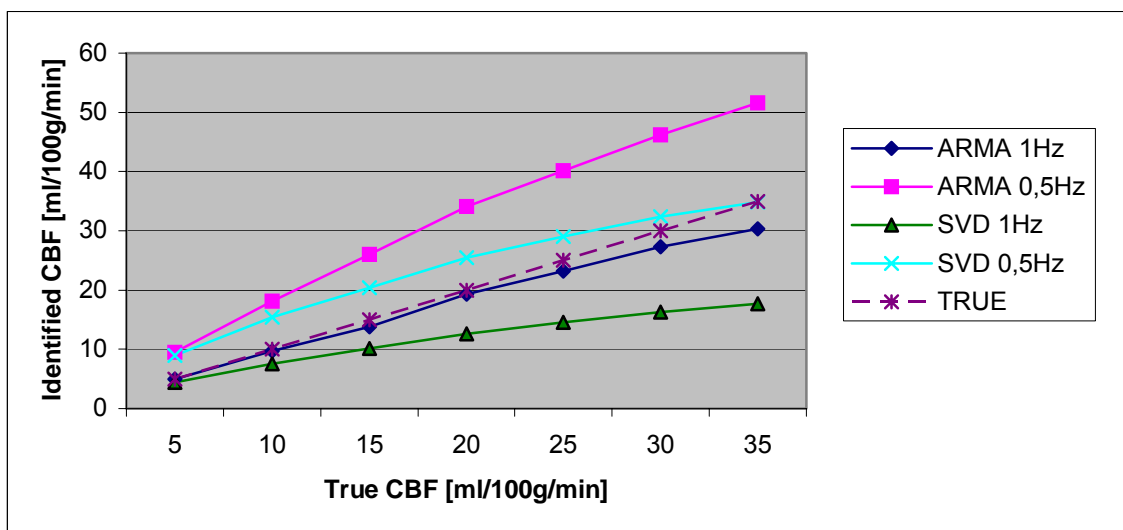


figure 16. Comparison of SNR shift sensitivity in blood flow estimation for both deconvolution methods. $CBV = 2\%$, $SNR_{tis} = 18$ dB and $SNR_{raif} = 15$ dB.

Specifically, the effect in the ARMA performance for a tissular SNR=18dB and an arterial SNR=15dB, for this sample rate shift, was similar to the simulation for $R_s=1$ Hz when the SNR was decreased. That means that the ARMA model passed from underestimation to overestimation when the sample rate was halved. For $R_s=0.5$ Hz the mean percentage estimation error was of 70%. This variation represents a mean relative increment of 0.4 in the initially identified flow with a sample rate of 1Hz. The ARMA standard variation increased in average 50%.

The SVD deconvolution passed from underestimation to overestimation as well, when the sample rate was changed to 0.5 Hz. This change represented a mean increment of 0.5 into the estimated flows for $R_s=1$ Hz. The standard variation for the SVD method increased in average 60 % in both blood volumes after the sample rate shift.

Noisy data in pixel simulation

Sensitivity to SNR shift:

When the random noise was increased (SNR_{tis} was changed from ROI to pixel level) the ARMA deconvolution passed from an MPE overestimation of 68% to 135%. Its mean standard deviation increased as well from 7.5 to 15.6 in other words there was a standard deviation increment of 108%.

On the other hand, SVD was less sensitive to the SNR shift, when the tissular signal-to-noise ratio was decreased to SNR_{tis}=6dB as seen in the following figure. The MPE passed from a mean percentage error of 32% to a MPE=35% with this SNR change. The mean SVD standard deviation passed from 3.7 to 5.

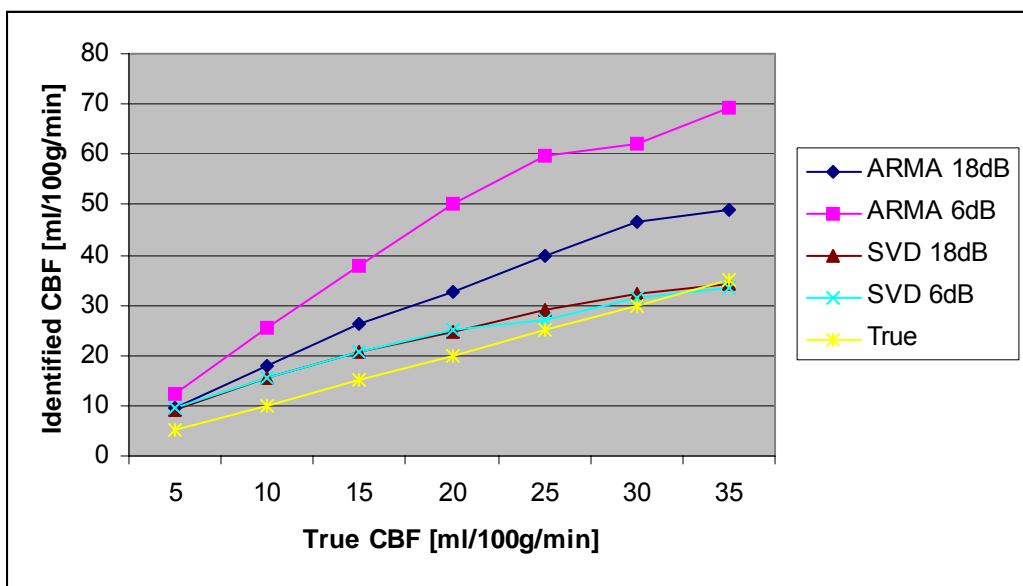


figure 17. Comparison of tissular SNR shift sensitivity in blood flow estimation for both deconvolution methods. $R_s = 0.5$ Hz and $SNR_{aif} = 15$ dB.

4.1.2. SVD and aSVD deconvolution

For a percentage threshold $P_{SVD} = 30\%$, the performance of the SVD method was not enhanced in terms of its mean percentage error, when the adaptive threshold deconvolution was used. The estimated flow was still underestimated in both blood volumes in the same proportions. For pixel and ROI simulations, neither the MPE nor the standard deviation was improved for both cerebral blood volumes. The reason for this lack of improvement was probably because the selected P_{SVD} was appropriate for the S/N ratio and therefore, the optimal oscillation index was already chosen in the SVD deconvolution.

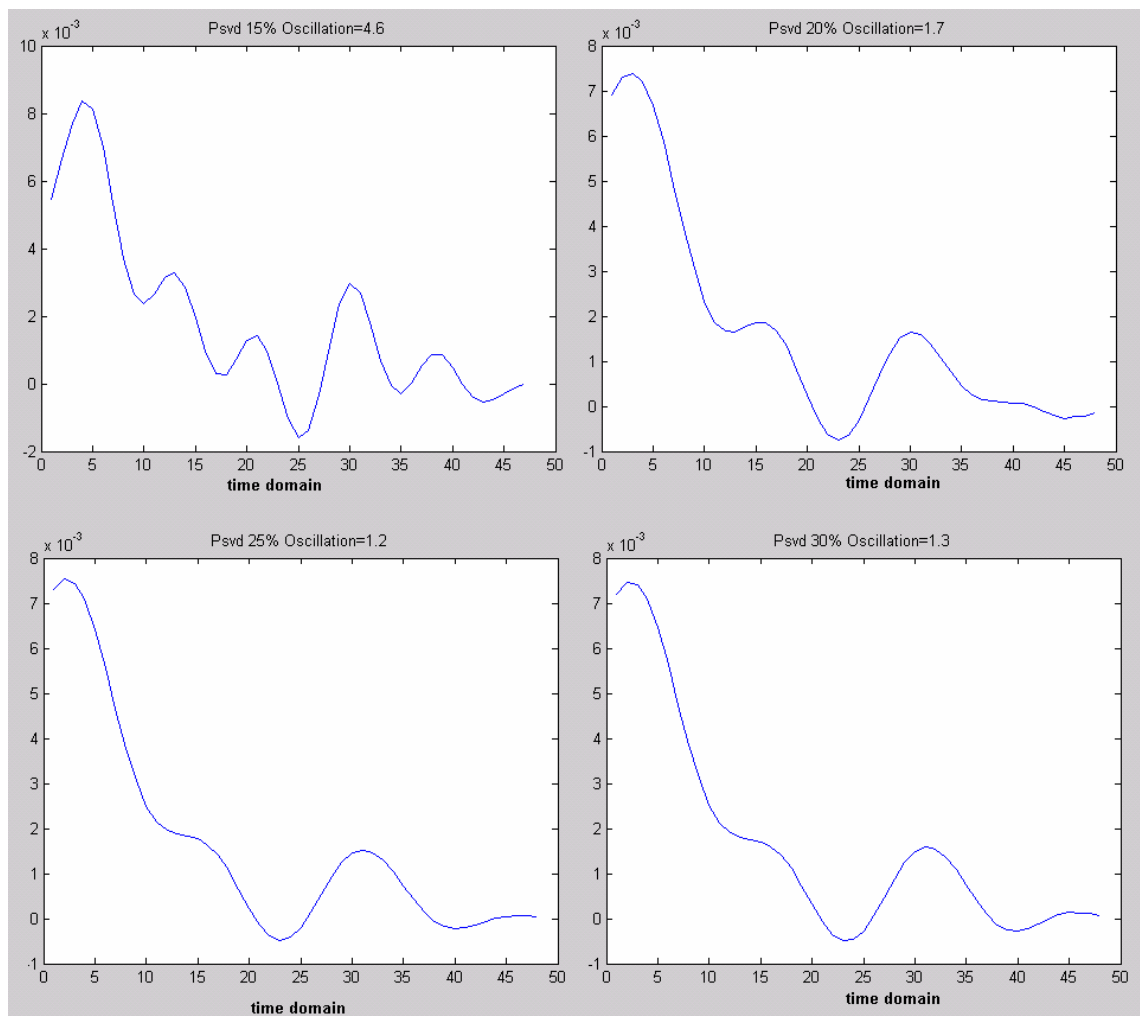


figure 18. Example of oscillation index calculation of four different residue functions from the adaptive SVD algorithm.

Under these noisy conditions, the main difference found between the basic SVD and aSVD deconvolution was in terms of its execution time. It is important to keep in mind that the aSVD algorithm needed to test 5 different matrix thresholds, recalculating at each time by deconvolution, the estimated residue function. Therefore aSVD was much more expensive in terms of execution time than SVD.

4.2. Perfusion MRI in stroke patients

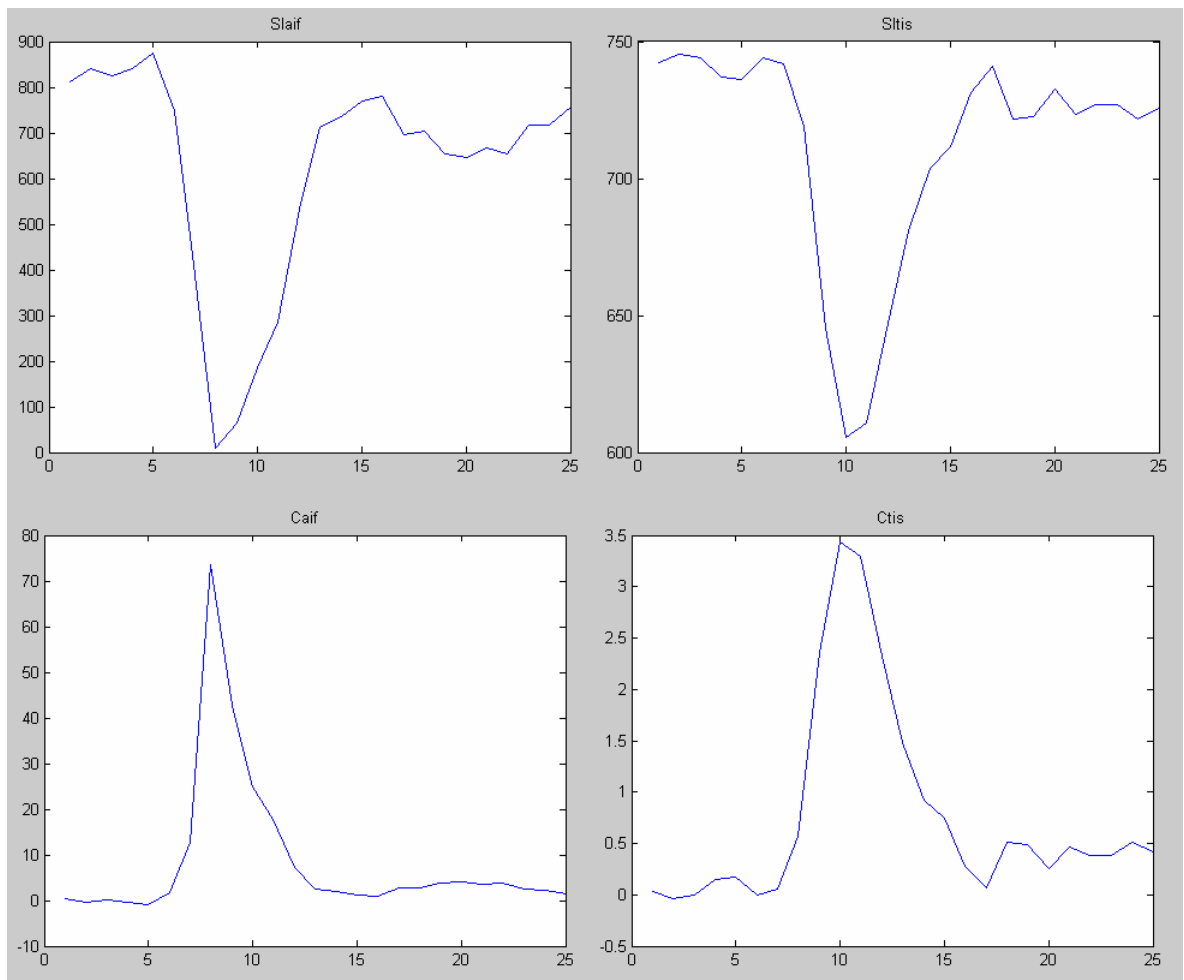


figure 19. Example of arterial and tissue concentrations calculated from SI functions for patient 6.

Due to the lack of a reference method for the assessment of perfusion, it was not possible to determine if there was under or overestimation for each case. However, this part of the experiment was useful to determine the orders of magnitude of the rCBF in clinical practice and to assess the relationship of the ARMA and SVD deconvolution.

A set of perfusion signals from one of the patients is shown in **figure 21** and its corresponding identified residue functions using both deconvolution methods are presented in the following figure.

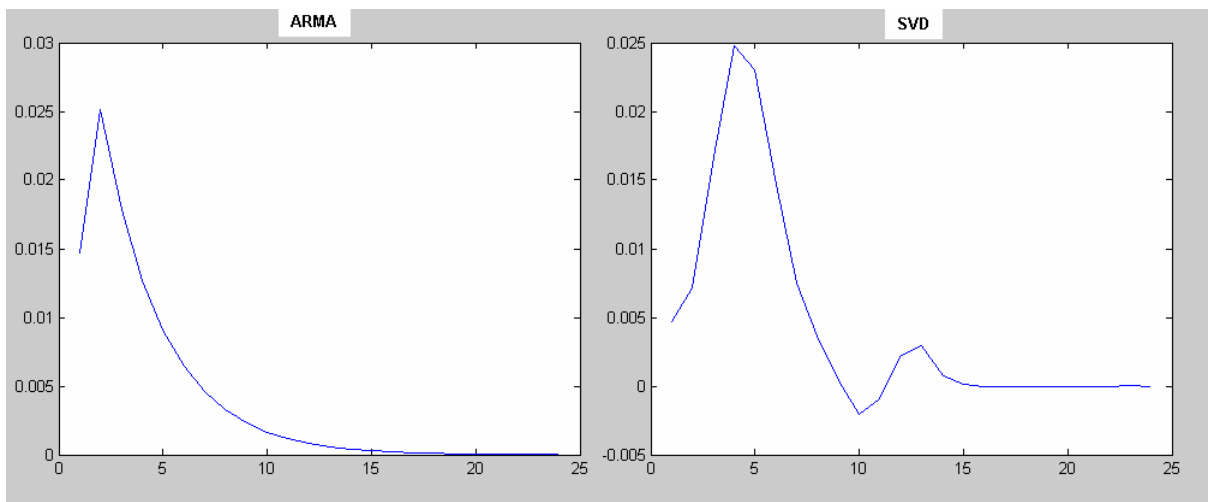


figure 20. Estimated residue function using the ARMA and SVD deconvolution model for patient 6.

Note that the residue function falls monotonically to zero in ARMA while the SVD function presents fluctuations over the time. The blood flow range in the 18 patients varied from 84 to 370 ml/min/100g in ARMA and from 43 to 300 ml/min/100g using SVD.

The clinically acquired human MRI data were coherent with the simulations since the estimated blood flow applying ARMA was in average 1.21 times greater than the SVD method. All the identified rCBF are summarized in the following figure:

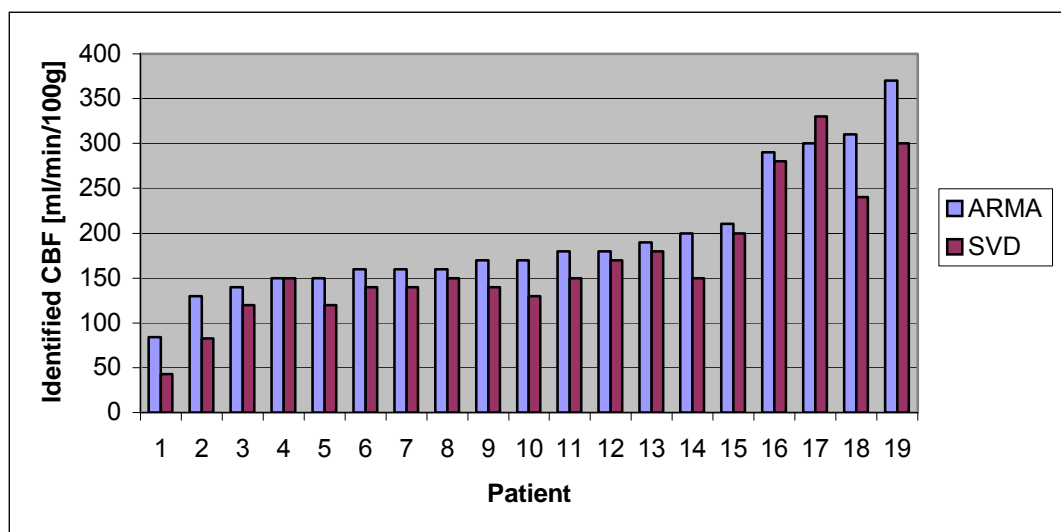


figure 21. Comparison of identified cerebral blood flow in 19 stroke patients using ARMA and SVD deconvolution.

Note that the real values of the regional cerebral blood flow are not shown in this figure. To obtain the true values it would be necessary to use a reference method such as the PET⁷ scan.

⁷ Positron Emission Tomography (PET)

5. CONCLUSIONS AND FURTHER WORK

5.1. CONCLUSIONS

The performances of the ARMA and SVD deconvolution method have been compared in ROI and pixel SNR, using two different sample rates. Monte-Carlo simulations and real clinical RM images were used during this work to determine the strengths and weaknesses of both algorithms. The simulation data was blurred with a realistic additive noise procedure and the results obtained were coherent with the flow estimation using the clinical data.

Satisfactory results in blood flow estimation using the ARMA model in previous studies encouraged the present work to apply this model into the cerebral context. The preceding tests [2] used experimental data from an isolated pig heart preparation due the similarities between the pig and human's heart. However, the estimation performance in the present circumstances, i.e., under less than myocardial flow conditions, was not the expected. The difference of the orders of magnitude between the brain and heart's flow changed the expected behavior of the ARMA method. However, each deconvolution method had its troubles depending on the application environment. This is why it is not desirable to search for the perfect deconvolution method, without knowing the context. Instead, the main question should be reformulated as:

Under which circumstances is it better to apply one algorithm instead of another?

Or, which is the most appropriate algorithm for some specific situation?

The ARMA deconvolution was generally closer to the true blood flow value than the SVD, when working with the higher sample rate and noise ratio. This signal to noise ratio corresponded respectively, to 18 dB and 15 dB for tissular and arterial concentration, i.e., a ROI selection. Therefore it is advisable to work with the ARMA model when working under these circumstances. Oppositely, it can be stated that ARMA estimation is not advisable when the blood flow is not greater than 100 ml/100g/minute with under-sampling (i.e., a sample rate of 0,5 Hz). This leads SI functions to be highly susceptible by random noise and therefore poor precision is found on regional cerebral blood flow identification.

The standard deviation in ARMA was generally greater than the SVD one. However, when the sample rate was halved, the increment of the SVD standard deviation was greater than the one of ARMA.

On the other hand, the singular values decomposition technique, showed to be less sensitive to SNR shifts. In other words, even if the SVD estimator was biased when the sample rate was of 1Hz it remained biased on the same proportions when the sample rate was of 0.5 Hz. Consequently, SVD is a suitable technique when the sample rate needs to be changed and if ROI or pixel selection is simultaneously being used.

The adaptive threshold deconvolution can be a useful method when the order of magnitude of the signal-to-noise ratio is unknown. Otherwise, this model is not advisable, since its execution time was much greater than the SVD deconvolution.

The simulations suggested that there is no difference in blood flow estimation in the two simulated volumes. In other words, the behavior of both deconvolution methods was very similar when dealing with healthy cerebral white or gray matter.

5.2. FURTHER WORK

The results from this study showed the influence of random noise in blood flow estimation and it was seen how strategies such as the ROI selection could optimize the rCBF identification. Further research could include regularization solutions to solve these kinds of discrete ill-posed problems. Different regularization strategies would be compared in order to determine the most appropriate technique for this MR perfusion-imaging context.

Knowing that the image of the patient is not completely motionless, it would be interesting to quantify the influence of image registration in the correct blood flow estimation.

The integration of both deconvolution methods into the software developed by the Cardiotools Creatis team is highly conceivable. Additionally, it would be attractive to prepare a synergetic deconvolution method. This fusion algorithm would automatically select the strengths of ARMA and SVD deconvolution, in order to produce a greater effect than the sum of their individual performances.

In this study, the ARMA deconvolution was applied using the first and second order for the poles and zeros models respectively. However, it would be interesting to see whether the rCBF estimation could be or not improved by changing the zeros model order.

REFERENCES

- [1] Wu O, Ostergaard L, Weisskoff RM, Benner T, Rosen BR, Sorensen AG. Tracer arrival timing-insensitive technique for estimating flow in MR perfusion-weighted imaging using singular value decomposition with a block-circulant deconvolution matrix. *Magn Reson Med*. 2003 Jul;50(1):164-74.
- [2] Neyran B, Janier M, Casali C, Revel D, Canet E. Mapping myocardial perfusion with an intravascular MR contrast agent: Robustness of deconvolution methods at various blood flows. *Magn. Reson Med*, 2002 ; vol 48, pp. 261-268.
- [3] Gobbel GT, Fike JR. A deconvolution method for evaluating indicator dilution curves. *Phys med Biol* 1994;39:1833-1854.
- [4] Liu H, Pu Y, Liu Y, Nickerson L, Adrews T, Fox P, Gao J. Cerebral blood flow measurement by dynamic contrast MRI using singular value decomposition with an adaptive threshold. *Magn. Reson Med* 42:167-172 (1999)
- [5] Smith M, Lu H, Frayne R. Signal-to-noise effects in quantitative cerebral perfusion using dynamic susceptibility contrast agents. *Magn. Reson Med* 49: 122-128 (2003)
- [6] Wiart M, Imagerie par résonance magnétique (IRM) de la perfusion cérébrale. Modélisation de la cinétique d'un produit de contraste pour la quantification de la perfusion. Thèse de doctorat, Lyon : Université Claude Bernard Lyon 1; 2000, pp.266

- [7] Wiart M, Rognin N, Berthezene Y, Nighoghossian N, Froment JC, Baskurt A. Perfusion-based segmentation of the human brain using similarity mapping. Magn. Reson Med, 2001 ; vol 45, n°2, pp. 261-268.
- [8] Carme S, Modélisation de la perfusion quantitative en imagerie par résonance magnétique (IRM) cardiaque in-vivo. Thèse de doctorat, Lyon : Ecole doctorale : Electronique, Electrotechnique Automatique ;2004.
- [9] Edelman R., Hesselink J., Zlatkin M., Clinical Magnetic Resonance Imaging. Volume One. 1996.
- [10] Ronald E. Walpole & Raymond H. Myers, Probability and statistics for engineers and scientists. New York : Macmillan, 1978
- [11] Robert R. Edelman, Michael B. Zlatkin, John R. Hesselink, Clinical magnetic resonance imaging. Volume 1. Philadelphia : W.B. Saunders, 1996